

Effect of Iron Doping on Structural, Optical and Magnetic Properties of TiO₂ thin films by Sol-gel Technique

Aseya Akbar¹⁾, Saira Riaz²⁾ and Shahzad Naseem²⁾

Centre of Excellence in Solid State Physics, University of the Punjab, Lahore, Pakistan

^{*)} saira_cssp@yahoo.com

ABSTRACT

During the past few years Titania (TiO₂) has attracted worldwide attraction due to its high refractive index and high value of dielectric constant. Doping of Titania with 3d metal ions is not only improves its spectral response in the visible region but also has a tremendous effect on its electrical properties. The substitution of Ti⁺⁴ ion with Fe⁺³ modifies intrinsic properties of TiO₂ such as its electrical, optical properties, surface morphology and grain size distribution. Ti⁺⁴ acts as charge compensator and electron donor and moreover, because of the presence of different phases Fe-doped TiO₂ can exhibit both n and p type conductivity. However, among various factors we are interested in enhancement of conductivity and optical properties of Fe-substituted TiO₂. So in order to study the effect of Fe doping on TiO₂, iron oxide was prepared using the sol-gel route reported earlier (Riaz 2013) and mixed in different ratios with TiO₂ prepared by sol-gel method. Films were then spin coated on glass and copper substrate. XRD results show high crystallinity of Fe₂O₃ and TiO₂ thin films and effect of iron substitution leads to decreased crystallinity. The films show high transparency in the visible region which is an important requirement for the films to be used as window layer in solar cells. TiO₂ is a wide band gap material and with metal doping its band gap decreases with increase in iron content.

1. INTRODUCTION

Many Among various materials of interest in spintronic as well as photovoltaic applications iron oxide is one of the most promising candidate. Iron oxide exist in three stoichiometric forms namely magnetite (Fe₃O₄), maghemite (γ-Fe₂O₃) and hematite (α-Fe₂O₃) (Yanagihara 2013). Among these important phases magnetite and maghemite both has cubic inverse spinel structure with the difference that there are vacancies present on the octahedral site in γ-Fe₂O₃ due to absence of Fe⁺² cations. Magnetite exhibit half metallicity at room temperature whereas, maghemite is a semiconductor at

¹⁾ Graduate Student

²⁾ Professor

room temperature. On the other hand hematite crystallizes in hexagonal corundum structure. It is also a semiconductor at room temperature with band gap of $\sim 2.1\text{eV}$ (Garcia 2013, Al-Kuhaili 2012).

Another material of interest in photovoltaic applications is Titanium dioxide (TiO_2). It is a n-type semiconductor with band gap of 3.2eV (Kemmitt 2013). Titania exists in three different crystallographic phases i.e. anatase, rutile and brookite. Anatase and rutile crystallizes in tetragonal phase where as brookite has orthorhombic phase (Moser et al. 2013). Other advantages of TiO_2 include its high refractive index and high dielectric constant. But due to its large band gap (lying in ultra-violet region) it can absorb only small portion of solar spectrum (Wu 2012).

During the past years, interest has arisen in TiO_2 substituted Fe_2O_3 not only due to the band gap engineering of Ti-doped Fe_2O_3 but also due to its ferromagnetic and photocatalytic applications (Wang 2009, Lu 2008, Flak 2013). Iron ions, Fe^{+3} , has octahedral radius of 0.079nm and Ti^{+4} has radius of 0.075nm so Ti^{+4} can be easily incorporated in host Fe_2O_3 lattice where it acts as an electron donor increasing the conductivity of Fe_2O_3 . Moreover it also helps in charge balance between Ti^{+4} and Fe^{+3} cation. Furthermore, Ti-doped Fe_2O_3 can be either n-type or p-type depending on the different phase compositions (Carneiro 2009, Babic 2012).

Effect of Ti^{+4} substitution in Fe_2O_3 and/or Fe^{+3} substitution in TiO_2 is studied by many researchers. Flak (2013) observed that Ti^{+4} doping favors the formation of $\alpha\text{-Fe}_2\text{O}_3$ instead of $\gamma\text{-Fe}_2\text{O}_3$ and in order to preserve charge neutrality Fe^{+3} cations are converted to Fe^{+2} cations. Further they observe that un-doped Fe_2O_3 shows p-type conductivity where as TiO_2 doping gives n-type characteristic. Bennaceur (2012) observed anatase to rutile transformation when the concentration of Fe^{+3} cation was increased from 10% to 20%. Also Fe^{+3} dopant not only decreases the anatase to rutile transition temperature but also lowers the band gap. Lin (2012) observed decrease in indirect optical band gap from 3.36eV to 2.95eV with increase in Fe^{+2} content to 7%. Shi (2012) studied the effect of different sintering atmospheres on iron doped TiO_2 gels. They observed the formation of Fe_2O_3 precipitates in oxidizing atmosphere where as reducing atmosphere increases the transition temperature of anatase to rutile. Sakai (2013) observed mixed valence states of +2 and +3 of iron in Fe-doped $\text{TiO}_{2-\delta}$ thus giving rise to room temperature ferromagnetism in TiO_2 .

We report the structural, electrical and optical properties of TiO_2 thin films. Moreover the effect of iron ion doping in TiO_2 films is taken into account with concentration varying from 0 ($x=0.0$) - 50% ($x=0.5$) in an interval of 10% ($x=0.1$ interval).

2. EXPERIMENTAL DETAILS

The Iron oxide sol was prepared using Iron chloride ($\text{FeCl}_3 \cdot 9\text{H}_2\text{O}$) that was dissolved in de-ionized water. Ethanol was used as a solvent where as ammonium hydroxide was used as gelation agent. The details of sol-gel synthesis of iron oxide are reported earlier by Riaz (2013). In order to prepare Titania by sol-gel method titanium tetrachloride (TiCl_4) was used as a precursor. TiCl_4 was mixed in ethanol keeping the molar ratio 1/1. The solution was added then drop wise to solution containing acetic acid and water kept at 5°C under constant nitrogen flow. The solution was stirred and heated in a water bath at 60°C . The two of the sols were then mixed together to

vary the concentration of iron ion from 0.0-0.5. The films were deposited on glass substrate with thickness of 200nm using spin coating method. The films were further annealed at 300°C in vacuum in the presence of magnetic field.

The crystallographic structure of doped and undoped thin films is studied using Bruker D8 Advance X-ray Diffractometer. M-2000 Variable Angle Spectroscopic Ellipsometer was used to study the optical properties such as refractive index, band gap. Lakeshore's 7404 Vibrating Sample Magnetometer (VSM) was used to study the magnetic properties of the films.

2. RESULTS AND DISCUSSION

Fig. show X-ray Diffraction patterns for undoped and iron (Fe) doped TiO₂ thin films. All the films show high degree of crystallinity. All of the high intensity peaks are indexed according to tetragonal rutile phase (JCPDS card no. 88-1175). However some contributions from brookite phase (JCPDS card no. 76-1937). The peaks with in $2\theta = 45^\circ$ - 50° and 67° - 70° are indexed according to brookite phase of titania. Diffraction peaks corresponding to iron are completely absent from the pattern indicating that iron has been successfully incorporated in titania host lattice.

It can be seen in Fig 1 that with increase in iron content the peaks shift to slightly higher angles. As the dopant concentration is increased to 30% the crystallinity of the films increases indicated by increase in peak intensities where as further increasing the dopant concentration reduces the peak intensities. At dopant concentration of 30% the strengthening of brookite phase is observed as a peak corresponding to brookite plane (102) emerged with high intensity. Whereas further increasing the dopant concentration suppresses the presence of brookite phase.

One of the most important things is that all of the films are oriented along (101) plane of rutile phase where as when the dopant concentration was increased to 50% not only the brookite phase is suppressed to a large extent but also the preferred orientation changes from (101) plane to (110) plane.

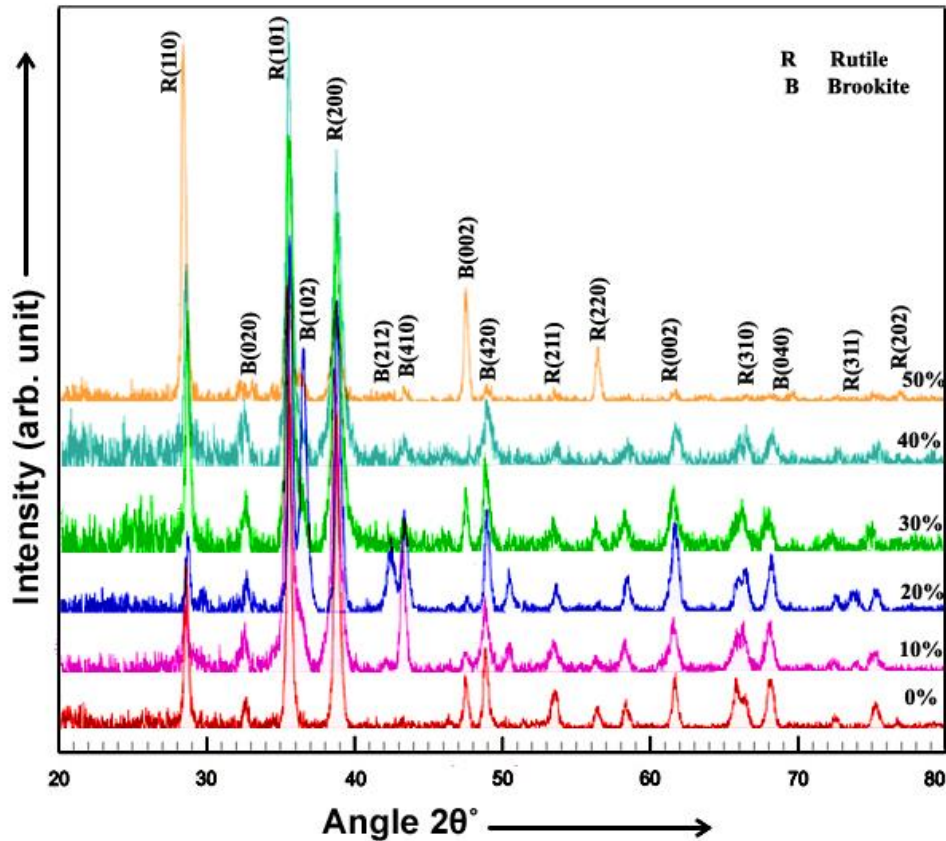


Fig. 1 XRD pattern for iron doped TiO₂ thin films

Fig. 2 show transmission curves for undoped and Fe doped TiO₂ thin films. The films are highly transmitting in the visible and infrared region. Undoped titania film show transmission of greater than 60% in the visible region. However, with 20% Fe doping the transparency of the films increased to more than 80%. Further increasing the dopant concentration reduces the transmission.

The band gaps of the titania with and without dopant films was calculated using Eq. 1.

$$\alpha = \frac{1}{t} \ln \frac{1}{T} \quad (1)$$

Where, *t* is the films thickness calculated using spectroscopic Ellipsometer and *T* is the transmission of the films. The band gaps are then found by extrapolation of linear region of α^2 vs. energy curve on the energy axis as shown in Fig. 3. The inset of Fig. 3 show variation of band gap with dopant concentration and it can be seen that the band gap of the films was decreased as the dopant concentration was increased to 40%. Further increase in dopant concentration increases the band gap. The band gap values of undoped titania and titania with 10%, 20%, 30%, 40% and 50% are found to be 3.38eV, 3.29 eV, 3.24 eV, 3.19 eV, 3.15 eV and 3.35eV respectively. The decrease of band gaps is attributed to the formation of localized states within the forbidden band near the conduction or valence band edge.

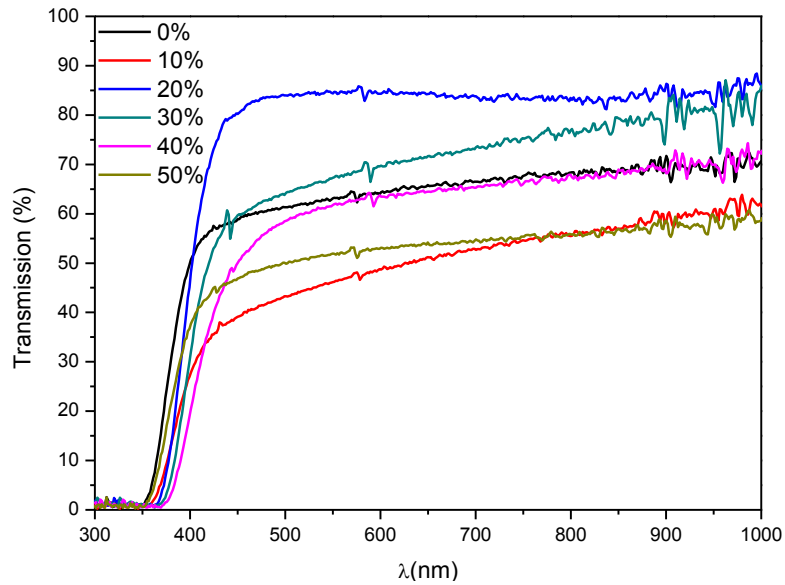


Fig. 2 Transmission as a function of wavelength for Fe doped TiO₂

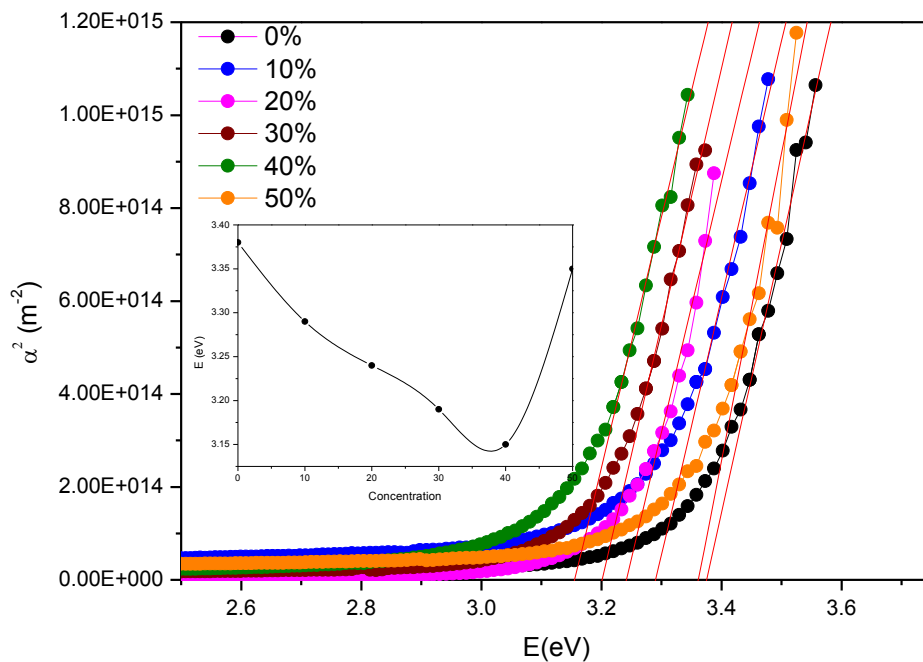


Fig. 3 α^2 vs. E(eV) for Fe doped TiO₂ films

The refractive index and extinction coefficient were found by fitting of experimental data obtained from Variable Angle Spectroscopic Ellipsometer (VASE) to obtain Mean Square Error (MSE) less than 1. The model used for fitting the experimental data within the transparent spectral region is Cauchy model. Fig. 4 show refractive index and extinction coefficient of Fe doped TiO₂ thin films. Both refractive index and extinction coefficient show normal dispersion behavior. High value of refractive index indicates

dense film structure. The refractive index decreases as the dopant concentration is increased from 0% to 30%. As the dopant concentration is further increased beyond 40% the refractive index increases. The sharp drop in extinction coefficient indicates the onset of optical absorption in titania thin films.

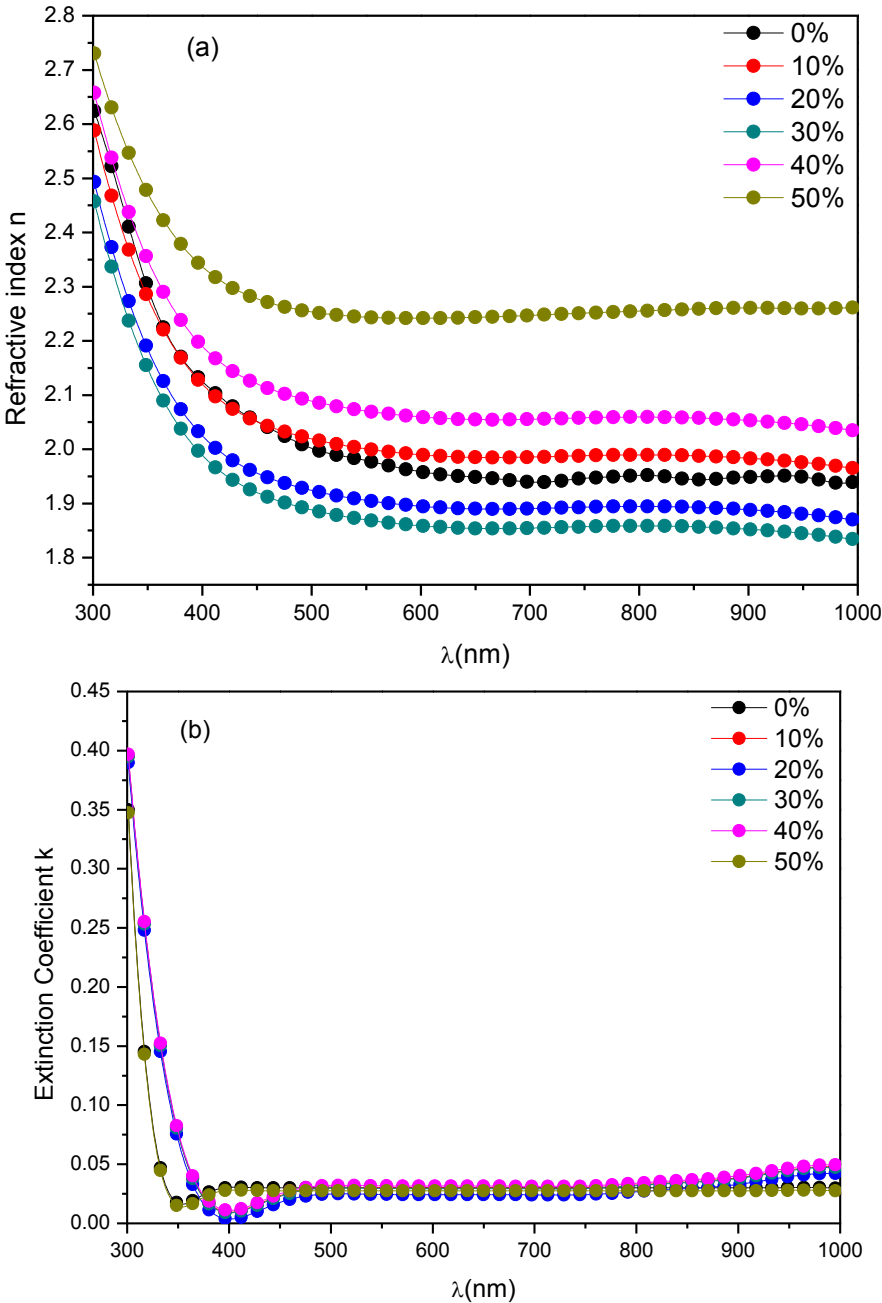


Fig. 4 (a) Refractive index (n) (b) Extinction coefficient (k) as a function of wavelength for various Fe concentrations in TiO₂ films

3. CONCLUSIONS

Iron doped TiO₂ thin films are prepared using sol-gel method. The films are highly crystalline and show the formation of rutile phase along with some contribution from brookite phase. The films are oriented along (101) plane however with 50% iron concentration the preferred orientation changed from (101) plane to (110) plane. The iron content also suppresses the brookite phase to some extent. The films are highly transparent in the visible and infrared region with band gaps in the range of 3.38-3.19eV. The high refractive index indicates that the films are highly dense.

REFERENCES

- Al-Kuhaili, M.F., Saleem, M. and Durrani, S.M.A. (2012), "Optical properties of iron oxide (α -Fe₂O₃) thin films deposited by the reactive evaporation of iron", *J. Alloy. Comp.*, **521**, 178–182.
- Babic, B., Gulicovski, J., Mitrovic, Z.D., Bucevac, D. Marija Prekajski, M., Zagorac, J. and Matovic, B. (2012), "Synthesis and characterization of Fe³⁺ doped titanium dioxide nanopowders", *Ceram. Int.*, **38**, 635–640.
- Bennaceur, J., Mechiakh, R., Bousbih, F., Jaouadi, M. and Chtourou R. (2012), "Effect of annealing temperatures and of high content of the iron ion (Fe³⁺)-doping on transition anatase–rutile phase of nanocrystalline TiO₂ thin films prepared by sol–gel spin coating", *J. Sol-Gel Sci. Technol.*, **61**, 69–76.
- Carneiro, J.O., Teixeira, V., Martins, A.J., Mendes, M., Ribeiro, M. and Vieira, A. (2009), "Surface properties of doped and undoped TiO₂ thin films deposited by magnetron sputtering", *Vacuum*, **83**, 1303–1306.
- Flak, D., Braun, A., Vollmer, A. and Rekas, M. (2013), "Effect of the titania substitution on the electronic structure and transport properties of FSS-made Fe₂O₃ nanoparticles for hydrogen sensing", *Sens. Actuators B*, <http://dx.doi.org/10.1016/j.snb.2012.12.038>.
- Garcia, H.A., Melo Jr., R.P., Azevedo, A. and Araujo, C.B. (2013), "Optical and structural characterization of iron oxide and cobalt oxide thin films at 800 nm", *Appl. Phys. B*, **111**, 313–321.
- Kemmitt, T., Al-Salim, N.I., Lian, J., Golovko, V.B. and Ruzicka, J.Y. (2013), "Transparent, photocatalytic, titania thin films formed at low temperature", *Curr. Appl. Phys.*, **13**, 142-147.
- Lin, C.Y.W., Channei, D., Koshy, P., Nakaruk, A. and Sorrell, C.C. (2012), "Effect of Fe doping on TiO₂ films prepared by spin coating", *Ceram. Int.*, **38**, 3943–3946.
- Lu, C.H., Hu, C.Y. and Wu, C.H. (2008), "Low-temperature preparation and characterization of iron-ion doped titania thin films", *J. Hazard. Mater.*, **159**, 636–639.
- Moser, E.M., Chappuis, S. and Olleros, J. (2013), "Production of photocatalytically active titania layers: A comparison of plasma processes and coating properties", *Surf. Coat. Technol.*, <http://dx.doi.org/10.1016/j.surfcoat.2013.01.050>.
- Riaz, S., Akbar, A. and Naseem, S. (2013), "Structural electrical and magnetic properties of iron oxide thin films," *Adv. Sci. Lett.*, **19**, 828-833.

- Sakai, E., Amemiya, K., Chikamatsu, A., Hirose, Y., Shimada, T. and Hasegawa, T. (2013), "X-ray absorption and magnetic circular dichroism characterization of Fe-doped $\text{TiO}_{2-\delta}$ thin films," *J. Magn. Magn. Mater.*, **333**, 130-133.
- Shi, Z.M. and Wang, X.H. (2012), "Phase transformation of titania gels highly doped with Fe in different sintering atmospheres", *Mater. Chem. Phys.*, **134**, 925-931.
- Wang, M.C., Lin, H.J. and Yang, T.S. (2009), "Characteristics and optical properties of iron ion (Fe^{3+})-doped titanium oxide thin films prepared by a sol-gel spin coating", *J. Alloy. Compd.*, **473**, 394-400.
- Wu, Q.L., Subramanian, N., Strzalka, J., Zhang Jiang, Z. and Rankin, S.E. (2012), "Tuning the mesopore structure of 3D hexagonal thin films using butanol as a co-solvent", *Thin Solid Films*, **520**, 3558-3566.
- Yanagihara, H., Myoka, M., Isaka, D., Niizeki, T., Mibu, K. and Kita, E. (2013), "Selective growth of Fe_3O_4 and $\gamma\text{-Fe}_2\text{O}_3$ films with reactive magnetron sputtering", *J. Phys. D: Appl. Phys.*, **46**, 175004.